### SES 2025

Twenty-first International Scientific Conference SPACE, ECOLOGY, SAFETY 21-25 October 2025, Sofia, Bulgaria

# SOME OBSERVATIONAL EFFECTS DURING SELECTED TIME-INTERVALS OF THE Z CAM STAR SY CNC

### Denislav Rusev, Daniela Boneva, Krasimira Yankova

Space Research and Technology Institute - Bulgarian Academy of Sciences e-mail: drusev@space.bas.bg, danvasan@space.bas.bg, f7@space.bas.bg

**Keywords:** Stars: Binary stars; Stars: cataclysmic variables; Accretion processes

**Abstract:** In our study, we present some observational effects during particular time-intervals of the Z Cam star SY Cnc. We use data from TESS (The Transiting Exoplanet Survey Satellite) and AAVSO (American Association of Variable Star Observers) international database, and we show some typical behaviors of this star. Fluctuations in brightness are detected in the light curves of SY Cnc, obtained from both astronomical facilities. The results show that the star passes through more active and less active states. Based on the observational data, we calculate the color indices and color temperature of the star during the outburst states. The radii of the primary and secondary components of the binary, and the orbital separation are also calculated. We apply our theoretical model to construct the effective temperature profiles in the accretion disc. After analysis of the SY Cnc parameters, we can confirm that with some exceptions the star is typical for the class of Z Cam stars.

# НЯКОИ НАБЛЮДАТЕЛНИ ЕФЕКТИ В ИЗБРАНИ ВРЕМЕВИ ИНТЕРВАЛИ НА Z CAM ЗВЕЗДАТА SY CNC

## Денислав Русев, Даниела Бонева, Красимира Янкова

Институт за космически изследвания и технологии – Българска академия на науките e-mail: drusev @space.bas.bg, danvasan @space.bas.bg, f7 @space.bas.bg

Ключови думи: Звезди: Двойни звезди; Акреция: акреционни дискове

**Резюме:** В нашето изследване представяме някои наблюдателни ефекти в определени времеви интервали на звездата SY Cnc (Cancer) от типа Z Cam. Използваме данни от международните бази данни TESS (The Transiting Exoplanet Survey Satellite) и AAVSO (American Association of Variable Star Observers), чрез които показваме някои типични поведения на тази звезда. В получените криви на блясъка от двата астрономически източника се детектират променливости в яркостта на SY Cnc. Резултатите показват наличие на по-активни и по-малко активни състояния, през които преминава звездата. На базата на данните от наблюденията, изчисляваме цветните индекси и цветната температура на звездата по време на състоянията с максимален блясък. Получените стойности показват преходи на обекта от по-студен към по-горещ и обратно.

Пресметнати са радиусите на първичния и вторичния компонент на двойната система, както и орбиталното разстояние между тях. Приложен е теоретичен модел за конструиране на профилите на ефективните температури в акреционния диск. След анализ на параметрите на SY Спс можем да потвърдим, че с някои изключения звездата е типична за класа на звездите от групата Z Сат.

## Introduction

Cataclysmic variables (CVs) are known as binary stars in which the matter transfers from the main-sequence secondary component to the white dwarf primary through the Roche lobe overflow [23]. One important characteristics of all cataclysmic variables is the presence of a compact object, in this case a white dwarf star. Another important feature of these stars is that they undergo accretion processes which may cause eruptions.

According to their behavior CVs can be divided into four classes [23]: Novae; Recurrent Novae; Nova-like stars; Dwarf Novae.

Novae stars are binary stars which explode regularly. Novae stars are thought to be "new" stars but later it was realized that they are binary stars which erupt [5]. Recurrent novae are a much smaller class of cataclysmic variables. It is thought that there are only 10 in our Galaxy. This is the main difference from Novae stars. Another difference is that they erupt more rarely than the Novae stars [14]. Another sub-class of cataclysmic variable stars are nova-like stars. Their most outstanding characteristics is the lack of outbursts [11]. Dwarf Novae are another subclass of cataclysmic variables. They are divided into three subtypes: U Gem, Z Cam and SU Uma stars. U Gem stars do not show very regular outbursts which distinguishes them from Z Cam stars. The later show frequent outbursts followed by periods of standstills. During outbursts the magnitude changes from 2 to 6 [16]. We will analyze in detail one member of this subtype of stars - SY Cnc further in the text. The third type of Dwarf-novae is SU Uma stars. The long-lasting super-outbursts is the typical feature of this type of stars. They can last around two weeks and are followed by normal outbursts [22].

Z Cam stars are among the most active stars comparing to the other subclasses of dwarf novae. Only SU Uma stars are more active because of its outbursts and super-outbursts. It makes them interesting for investigation. One of the typical Z Cam star is SY Cancer (Cnc). It is a comparatively bright star with its maximum brightness of 11 magnitude [15] and in its minimum of 14 mag in V band [15]. An estimation of the orbital period gives  $\approx$  0.382 days [15]. The outburst period is 27 days [4]. SY Cnc passes through periods of outbursts and standstills. During outburst the star's maximum magnitude is 11. Standstills' time-periods are connected with lower magnitudes. The blackbody temperature of SY Cnc is estimated as  $\approx$  11000K [13]. The distance to the object is  $\approx$  405 pc [6]. An interesting feature of this object is the mass of the companion star, which is around the solar mass. It is untypical for the Z Cam stars [21]. The estimated values of masses are M1wd = (0.42  $\pm$  0.12) M $_{\odot}$  and M2 = (0.23  $\pm$  0.05) M $_{\odot}$  [21] and M1wd = (0.65 - 1.31) M $_{\odot}$  and M2 = (0.77 - 1.54) M $_{\odot}$  [4].

It is stated that the accretion disc that is formed around Z Cam stars is stable at certain temperatures and critical accretion rate  $\dot{M}crit$ . If the effective temperature of the disc is above 8000 K and below 6000 K the disc is in a stable state. If the accretion rate is below a certain amount, the star passes through periods of outbursts and standstills [10]. More accurately, if the accretion rate is above critical, there is a stable state of standstill. If the accretion rate is below critical, there are outbursts [6].

The observational data for SY Cnc, obtained both from TESS (The Transiting Exoplanet Survey Satellite) and AAVSO (American Association of Variable Star Observers), are reported in the next Section. Based on observations, we derive the color indices and color temperatures at maximum brightness, also some parameters of the binary system, as radius of the primary and secondary components, binary separation and the discs' effective temperatures profiles are calculated in the last Section.

## Observational data and results for SY Cnc

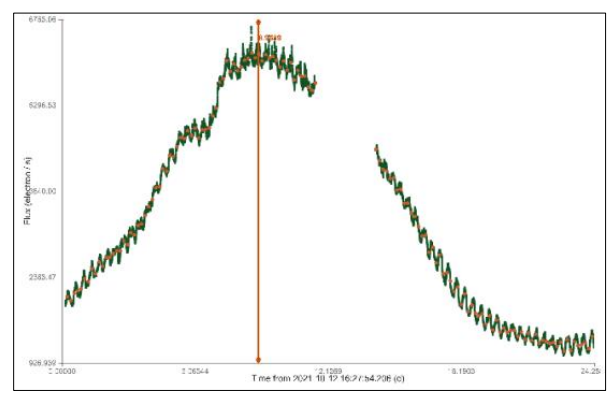
In this paper, we apply observational data obtained with different instruments and facilities, situated on board of TESS and AAVSO international database.

# Observational data and results from TESS

We use data from TESS observations, obtained from two sectors of the northern sky. The TESS main aim is to search for transiting Earth-sized exo-planets. Observations of bright stars, over 200 000 objects, are also provided [9]. The light curves of the studied objects by TESS photometric series could be analysed with a 2-minute cadence [8, 18].

The data of SY Cnc are obtained in the time-intervals: (2021-10-12 – 2021-11-05 Calendar dates, means yy-mm-dd), from the sector number 44, with an exposure time 120 sec and (2023-11-11 – 2023-12-07), from sector 72, with an exposure time 120 sec. The data were downloaded and reducing from the Mikulski Archive for Space Telescopes (MAST, https://archive.stsci.edu).

The light curves for both time-intervals (Figs. 1a and 2a) were constructed as Flux-rate [e-/s] (electrons/second) vs. time in [days], from the Simple Aperture Photometry (SAP) Flux data. Frequency analysis of the obtained data for the same time-intervals are represented as power-period diagrams (Figs. 1b and 2b). To determine the period, the Lomb-Scargle method is applied [12, 19].



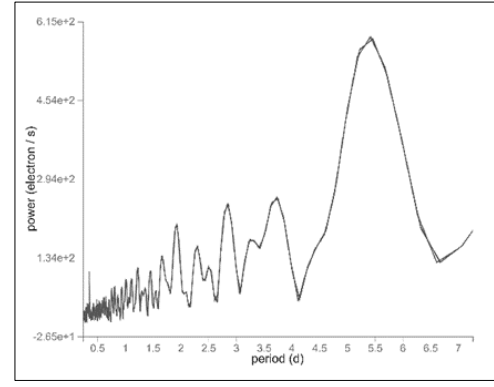
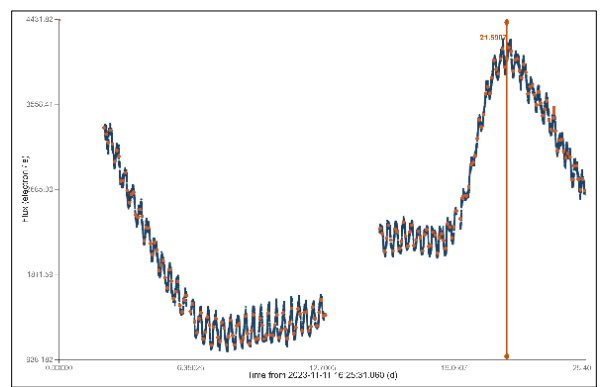


Fig.1. Light curve of SY Cnc, created with the data obtained from TESS for the observational interval 2459499.69 – 2459523.93 JD (a, left panel). The dotted red line denotes the binned curve with number of bins 200 for the optimal fit. The time of the peak in the flux variation is marked with a red vertical line. (b, Right panel): a power-period diagram of SY Cnc, obtained by the frequency analysis with data for the same observational time.



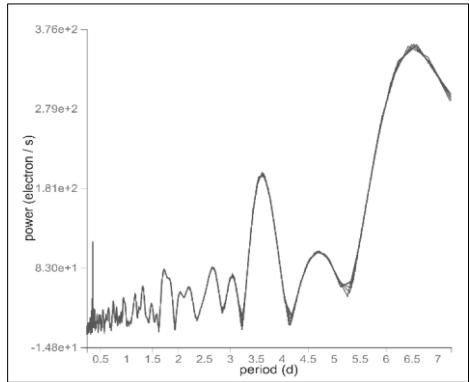


Fig. 2. Light curve of SY Cnc, created with the data obtained from TESS for the observational interval 2460259.68 – 2460285.085 JD (a, left panel). The time of the peak in the flux variation is marked with a red vertical line. The dotted red line denotes the binned curve with number of bins 150 for the optimal fit. (Right panel, b): a power-period diagram of SY Cnc, obtained by the frequency analysis data for the same observational time.

An increase in brightness is seen both in the flux vs. time curve and in the frequency analysis diagrams. The maximum values of the flux-rates of these light variations are  $(6.46 \pm 0.003) \times 10^3$  e/s with amplitudes of increasing of  $(2.25 \pm 0.003) \times 10^3$  e/s for the first time-interval.

During the second interval, the maximum observed flux-rates vs. time is estimated as  $(4.23 \pm 0.002) \times 10^3$  e/s, with amplitudes between minimum and maximum values of  $(3.09 \pm 0.004) \times 10^3$  e/s and the amplitude increased value is  $(2.05 \pm 0.03) \times 10^3$  e/s. This variation in brightness could be identified as a rapid burst activity. The appearance of small-scale oscillations is observed during the both observational time-intervals, with amplitudes of  $(0.21 - 0.38) \pm 0.003 \times 10^3$  e/s.

## • Observational data from AAVSO

The observational data obtained for SY Cnc in BVRI bands cover two observational time-intervals. The first one is in the range: 2458800-2459000 JD (Julian dates) (2019-11-12 - 2020-05-30 Calendar dates). In the obtained data we see irregular variations of brightness in time and between the minimum (13.32  $\pm$  0.022 mag in V band) and maximum (11.13  $\pm$  0.026 mag in V band) values it is in the range 10 - 15 days in average, with periodicity of 25 - 30 days (see Fig. 3a). The second interval is in a range: 2458000 - 2458300 JD (2017-09-03 - 2018-06-30 Calendar dates). We observe an increase in brightness in two consecutive peaks with a period between them of  $\approx$  32 days, the magnitude in its second, higher maximum is 11.12  $\pm$  0.018 in the V band (Fig. 3b).

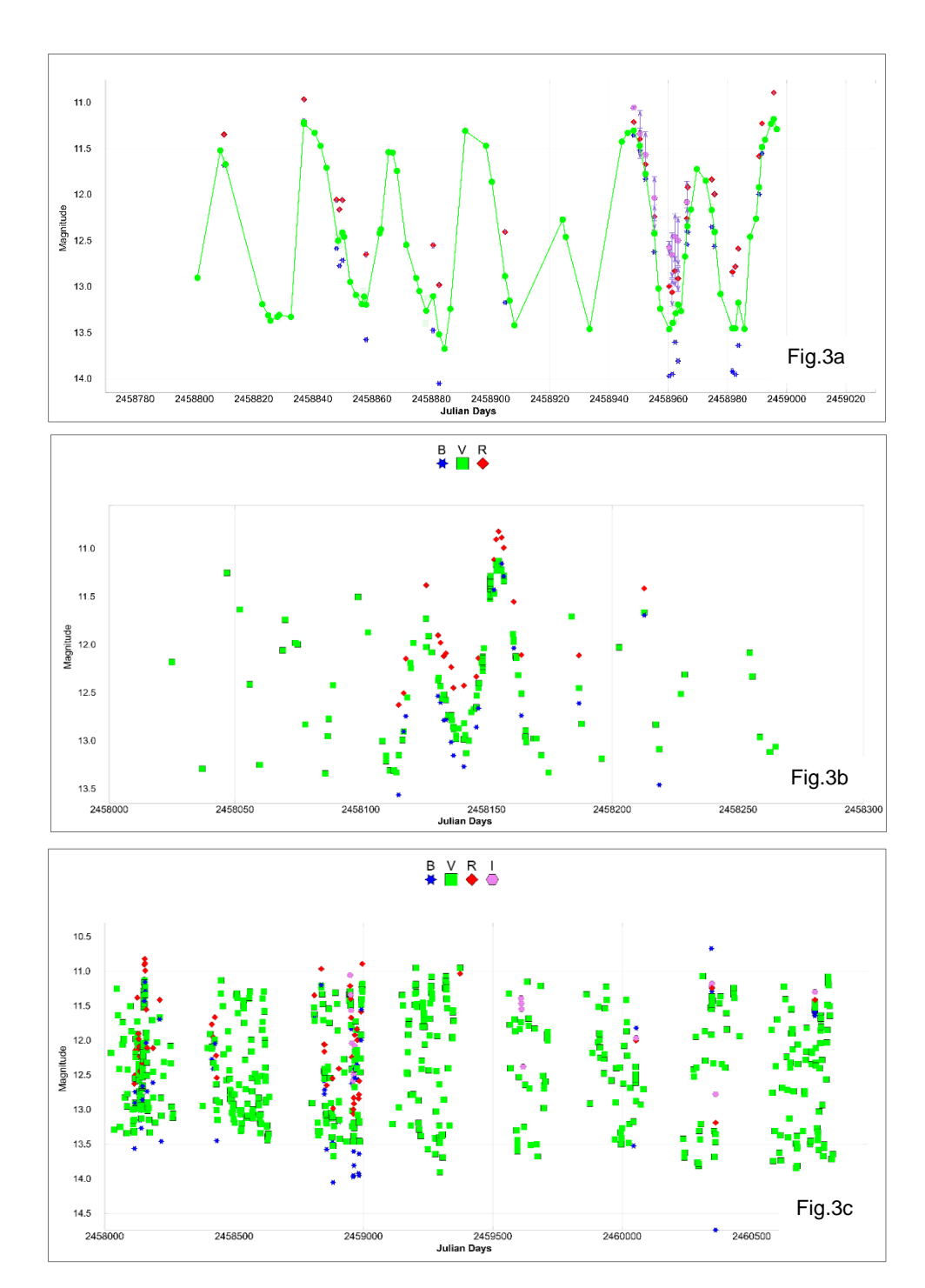


Fig. 3. Light curves of SY Cnc in BVRI bands for the intervals of time: 2019-11-12 – 2020-05-30 (3a) and 2017-09-03 to 2018-06-30 (3b) Calendar dates. Eight years interval of observations in BVRI bands (3c). The observational times in the figures are in JD (Julian dates). The data are taken from AAVSO.

We also present a light curve for a longer time-interval of observations (2458100–2460900 JD). The obtained observational data show the star's behavior stays in a similar way during the last  $\sim$  8 years. Its brightness varies in the range of 13.61–11.02 magnitudes in V band, with amplitude variations of 2.0 – 2.5 mag (Fig. 3c). In contrast with other Z Cams object, like Z Cam and AT Cnc (see Boneva et al. 2024 [2], where the light curves of the two states are seen very clearly), we cannot distinguish prolonged states of standstill and outbursts for this longer time light curve of SY Cnc.

## Parameters of the system and temperature profiles

## Radii of the two components and binary separation

In this section, we present our calculations of some system parameters of SY Cnc, as radii of the primary and secondary components and the distance between them.

To calculate the radius of the white dwarf primary R<sub>1</sub>, the Eggleton's mass-radius relation is convenient to apply (eq. 1).

(1) 
$$\frac{R_1}{R_{\odot}} = 0.0114 \left[ \left( \frac{M_1}{M_{Ch}} \right)^{-2/3} - \left( \frac{M_1}{M_{Ch}} \right)^{2/3} \right]^{1/2} \times \left[ 1 + 3.5 \left( \frac{M_1}{M_p} \right)^{-2/3} + \left( \frac{M_1}{M_p} \right)^{-1} \right]^{-2/3}$$

where  $M_{Ch}$  = 1.4 $M_{\odot}$  is the Chandrasekhar mass;  $M_{p}$  = 0.00057  $M_{\odot}$  is a constant.

We use two different values of the primary white dwarf star mass M1 (see Introduction), as obtained by Smith et al. (2005) [21], noted here as M1a = 0.42  $M_{\odot}$  and the minimum value from Casares et al. 2009 [4], as M1b = 0.65  $M_{\odot}$ , correspondingly.

Therefore, our calculations give two different values for the primary radius, R1a and R1b.

$$R_{1a} = (1.02 \pm 0.002) \times 10^9 \, cm = 0.014 \pm 0.002 \; R_{\odot}$$
 for M1a;  $R_{1b} = (7.95 \pm 0.004) \times 10^8 \, cm = 0.015 \pm 0.001 \; R_{\odot}$  for M1b.

To calculate the binary separation a the Kepler's 3rd law expression can be used (Eq. 2). We apply the same value for M1 and for M2 from [21], and again the minimum value from [4], noted here as M2a = 0.23 M $_{\odot}$  and M2b = 0.77 M $_{\odot}$ .

(2) 
$$a = \left(\frac{G(M_1 + M_2)M_{\odot}P_{orb}^2}{4\pi^2}\right)^{\frac{1}{3}}$$

Then, the obtained values for *a* are:

a1 = 
$$(1.31 \pm 0.01) \times 10^{11}$$
 cm =  $1.89 \pm 0.01$  R <sub>$\odot$</sub>   
a2 =  $(1.71 \pm 0.02) \times 10^{11}$  cm =  $2.47 \pm 0.002$  R <sub>$\odot$</sub> 

Further, to calculate the radius R2 of the secondary component of the objects, the equation of Eggleton [7], which gives a high accuracy of the obtained values, is applicable.

(3) 
$$\frac{R_2}{a} = \frac{0.49q^{\frac{2}{3}}}{0.6q^{\frac{2}{3}} + ln\left(1 + q^{\frac{1}{3}}\right)}$$

Here  $q = M_1/M_2$  is the mass ratio and in accordance with two values of M1 and M2, we have q1 = 1.82 ± 0.002; q2 = 0.84 ± 0.002. Then, for the radii R2a and R2b we obtain:

$$\begin{aligned} R_{2a} &= (2.97 \pm 0.03) \times 10^{10} \, \text{cm} = 0.431 \pm 0.004 \; R_{\odot} \\ R_{2b} &= (2.50 \pm 0.02) \times 10^{10} \, \text{cm} = 0.363 \pm 0.003 \; R_{\odot} \end{aligned}$$

All the values of the calculated parameters are given in Table 1.

Table 1. System parameters of SY Cnc, calculated in this paper, as follows:  $R_1$  – radius of the primary;  $R_2$  –radius of the secondary; a – binary separation

Parameters /Object: SY Cnc Masses	Rwd (R₁) [R⊙]	R₂ [R <sub>⊙</sub> ]	a [R <sub>⊙</sub> ]
M1a; M2a	0.014 ± 0.002	0.431 ± 0.004	1.89 ± 0.01
M1b; M2b	0.015 ± 0.001	0.363 ± 0.003	2.47 ± 0.002

## Color index and color temperature

The observational data from AAVSO in BVRI filters allow us to estimate the color indices of SY Cnc. Following the data, we obtain the color indices (B - V) with values of the magnitudes in B and V filters at maximum brightness for the two time-intervals separately. During the first observational time-interval (see previous Section), the obtained index for the night of 2458837.03 JD has a negative value (B - V =  $-0.035 \pm 0.022$ ), while on the night of 2458948.34 JD the color index is positive (B - V =  $0.036 \pm 0.016$ ). This is an indication that during these two outbursts the object became bluer and hotter and then redder and cooler in a frame of  $\sim 4$  months.

In the time-span of the second interval (Fig. 2b), during the outburst of the object the color varies from red to blue at its maximums in two nights. On the night of 2458154.80 JD the color index is positive (B - V =  $0.027 \pm 0.004$ ) and on the night of 2458156.00 JD is already negative (B - V =  $0.066 \pm 0.022$ ).

Further, using the more precise derredened color index  $(B - V)_0$ , we could calculate the color temperature  $T(B - V)_0$  of SY Cnc during the maximum brightness in both observational time-intervals. The formula of Ballesteros [1] is appropriate to apply here:

(4) 
$$(Tcol)_0 = 4600K \times \frac{1}{(0.92(B-V)_0 + 1.7)} + \frac{1}{(0.92(B-V)_0 + 0.62)},$$

According to Shara et al. 2012 [20], the color excess value of SY Cnc is E(B - V) = 0.0 [3]. Using this value and applying it on the expression E(B - V) = (B - V) - (B - V)<sub>0</sub>, we obtain that (B - V)<sub>0</sub>  $\approx$  (B - V)  $\pm$  0.0001. Then, our calculations give the next values for the color temperatures (also see Table 2):

$$(Tcol)_{0_{-}11} = 10584 \pm 425 \text{ K}; (Tcol)_{0_{-}12} = 9700 \pm 382 \text{ K}; (Tcol)_{0_{-}21} = 9800 \pm 470 \text{ K}; (Tcol)_{0_{-}22} = 11030 \pm 330 \text{ K}.$$

This result confirms that during the second observational time-interval the object became hotter, which is a sign of active accretion processes.

Table 2. Color index and color temperatures of SY Cnc during the two observational time-intervals. Values are obtained at maximum brightness for the selected dates

Object/ Values	Time-interval 2458800-2459000 JD		Time-interval 2458000 – 2458300 JD	
SY Cnc	(B-V) <sub>0</sub> _max	(Tcol) <sub>0</sub> _max [K]	(B-V) <sub>0</sub> _max	(Tcol) <sub>0</sub> _max [K]
<b>JD</b> 2458837.03		<b>JD</b> 2458154.80		
- 0.035 ± 0.022		10585 ± 425	0.027 ± 0.004	9800 ± 470
<b>JD</b> 2458948.34		<b>JD</b> 2458156.00		
0.03	36 ± 0.016	9700 ± 380	- 0.066 ± 0.022	11030 ± 330

## · Temperature profiles

Like other DN stars and as a member of Z Cams, an accretion disc around the white dwarf star is formed in the SY Cnc's binary configuration. The outbursts manifestation could be sometimes related to the disc's activity and temperature variations. In this section we use the next formula of Pringle [17] to show the development of the effective temperature (Teff) in the accretion discs of the object.

(5) 
$$T_{eff} = T_{wd} \left(\frac{R_{wd}}{r}\right)^{3/4} \left(1 - \left(\frac{R_{wd}}{r}\right)^{1/2}\right)^{1/4}$$

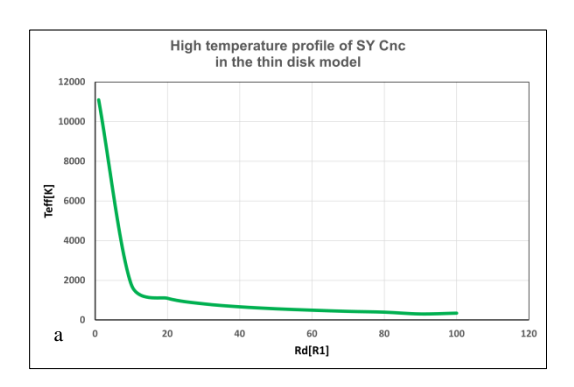
For this aim, we apply one-temperature model of an accretion disc. It is known that the disc develops an advection. In this case, a non-stationary and non-axisymmetric accretion flows are considered and advection stays in the non-dominant regime/mode. The model's results allow us to get 2D-structure of the disc [24]. Then the effective temperature in the terms of this solution is:

(6) 
$$T_{eff} = T_0 \left(\frac{x}{R_d}\right)^{1/4} (f_1 f_4 x (4x)^3)^{1/4}$$

Here x = r / Rd, Rd - accretion disc radius, f1(x) - equatorial density and f4(x) - disc half-thickness correspondingly. Then, the profiles have the form:

$$T_{eff} \approx 5 \left(\frac{10}{x}\right)^2 \left(2.7 (1-x)/x^{\frac{1}{2}}\right)^{\frac{1}{4}}$$

The solutions are obtained for both a thin disc model and an advective model (Fig. 4a and Fig. 4b).



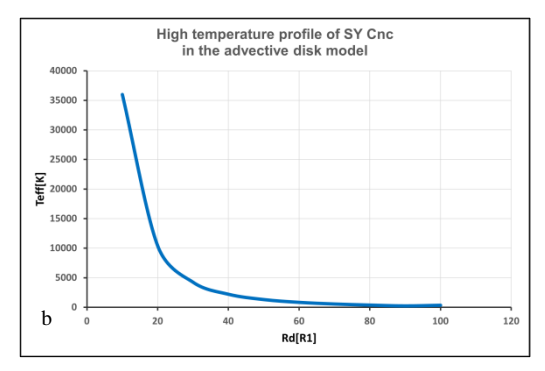


Fig. 4. The effective temperatures profiles of SY Cnc against the accretion disc's radius. Comparison of the two models' profiles is seen in 4(a) for the thin disc model and in 3(b) for the advective disc model.

Figures compare the changes of the disc temperature profile for the two models, for the surface temperature of the accretor of the SY Cnc. The effective temperatures are plotted against the discs' radii (Rd), where Rd is in a unit of white dwarf radius  $R_1$ . We used the averaged value of  $R_1$  from our calculations in previous subsections (Table 1). The result demonstrates that the advective model much better represents the relationship between the disc's level of activity and the compactness degree of the accretor.

#### Conclusion

In this paper, we presented our study of the Z Cam star SY Cnc. We use observational data from two observational facilities, TESS and AAVSO. The resulting light curves and the power-period diagrams from TESS show the activity in the object during the observational time-intervals. In the obtained light curves of SY Cnc from AAVSO, brightness variations with larger amplitudes are seen.

Based on the observational data, we estimated the color indices and color temperatures at their maximum brightness and vary in the ranges: -  $0.066 < (B - V)_0 < 0.036$ ;  $11030 [K] > T(B - V)_0 > 9700 [K]$ . According to the calculated values, during the two outbursts the object became bluer and hotter and then redder and cooler.

We calculated the radii of the primary and secondary components of SY Cnc, and the orbital separation between them. It is still under discussion, but because of its higher mass-ratio and the form of its temperature profile distribution with a higher color temperature, SY Cnc could have a sign of non-stable mass-transfer rate. We compared the parameters values of SY Cnc with two other Z Cam stars, Z Cam and AT Cnc, calculated in (Boneva et al. 2024, [1]). They have similar values of the parameters as masses, orbital periods and observational magnitudes.

We constructed the profiles of the effective temperature in the accretion discs of the object. From our analysis the known correlation is seen - the higher the temperature of the white dwarf, the smaller its radius. This confirms that the hotter object and its disc are definitely more active.

## Acknowledgments:

This paper includes data collected with the TESS mission, obtained from the MAST data archive at the Space Telescope Science Institute (STScI). Funding for the TESS mission is provided by the NASA Explorer Program. STScI is operated by the Association of Universities for Research in Astronomy, Inc., under NASA contract NAS 5–26555. The authors acknowledge with thanks the variable star observations from the AAVSO International Database contributed by observers worldwide and used in this research.

#### References:

- 1. Ballesteros, F.J., New insights into black bodies, Europhys. Lett., 2012, 97, 34008
- 2. Boneva, D., K. Yankova, D. Rusev, Periods of outbursts and standstills and parameters variations in two Z Cam stars: Z Cam and AT Cnc., Astronomy, MDPI, 2024, 3, 208–219
- 3. Bruch, A, Engel, A, A catalogue of UBV colours of cataclysmic variables., A&AS, 1994, Vol. 104, p.79-88
- Casares, J., I. G. Martínez-Pais, P. Rodríguez-Gil, SY Cnc, a case for unstable mass transfer?, MNRAS, 2009, Vol. 399, Issue 3, p. 1534–1538
- 5. Chomiuk, L., B. D. Metzger, K. J. Shen, New Insights into Classical Novae, ARA&A, 2021, Vol. 59:391-444
- DR3-Gaia Collaboration, Vallenari, A., A.G.A. Brown et al, A&A, 2023, 674, A1
- 7. Eggleton, P.P., Approximations to the radii of Roche lobes, ApJ, 1983, vol. 268, p. 368, 369
- 8. Gilbert, E.A., T. Barclay, E.V. Quintana et al., Flares, Rotation, and Planets of the AU Mic System from TESS Observations, AJ, 2022, 163, 147
- 9. Günther, M.N., Z. Zhan, S. Seager, et al., Stellar Flares from the First TESS Data Release: Exploring a New Sample of M Dwarfs, AJ, 2020, 159, 60
- Hameury, J.-M., J.-P. Lasota, Anomalous Z Cam stars: a response to mass transfer outbursts, A&A, 2014, 569, A48
- 11. Ladous, C., Nova-like variables, NASA, Washington, Cataclysmic Variables and Related Objects, 1993
- 12. Lomb, N.R., Least-squares frequency analysis of unequally spaced data, ApSS, 1976, 39, pp. 447-462
- 13. Middleditch, J., F. Cordova, The colors of the pulsations and flickering of SY Cancri during outburst, ApJ, 1982, 255:585-595
- 14. Mukai, K., Recurrent Novae a review, arXiv:1407.4526v1, 2014
- 15. Ohshima, T, Secular Variation in the Interval of Outbursts in Z Cam-type Dwarf Novae., Stars and Galaxies, 2022
- 16. Osaki, Y., Dwarf-nova Outbursts, PASP, 1996, 108 39
- 17. Pringle, J.E., Accretion discs in astrophysics, ARA&A., 1981, Volume 19 (A82-11551 02-90) Palo Alto, CA, Annual Reviews, Inc., p. 137–162
- 18. Ricker, G.R., J.N. Winn, R. Vanderspek, et al., Transiting Exoplanet Survey Satellite (TESS), Journal of Astronomical Telescopes, Instruments, and Systems, 2015, 1, id. 014003
- Scargle, J.D., Studies in astronomical time series analysis. II. Statistical aspects of spectral analysis of unevenly spaced data, ApJ, 1982, 263, 853
- 20. Shara,M, T. Mizusawa, P. Wehinger et al, AT Cnc: a second dwarf nova with a classical nova shell, ApJ, 2012, 758 121
- 21. Smith, R.; O. Mehes.; D. Vande Putte; N. Hawkins, A non-main-sequence secondary in SY Cancri., MNRAS, 2005, 360, 364–374
- 22. Vogt, N, The SU Uma stars an important sub-group of Dwarf Novae, A&A, 1980, vol. 88, no. 1-2, p. 66-76.
- 23. Warner, B., Transitions to and from Stable Discs in Cataclysmic Variable Stars., Astrophys. Space Sci., 1995, 230. 83–94
- 24. Yankova, Kr., Filipov, L., Structuring the hot advective accretion flow, as a result interaction of plasma with magnetic field, 40th COSPAR Scientific Assembly, 2014. http://adsabs.harvard.edu/abs/2014arXiv1408.4011Y